Investigation of the Mechanical Degradation of Zinc-Based Cold Spray Coatings for Steel Pipelines

Lucas Teeter
National Energy Technology Laboratory
1450 Queen Avenue SW
Albany, OR 97321, USA

NETL Support Contractor
1450 Queen Avenue SW
Albany, OR 97321, USA

Zineb Belarbi
National Energy Technology Laboratory
1450 Queen Avenue SW
Albany, OR 97321, USA

NETL Support Contractor
1450 Queen Avenue SW
Albany, OR 97321, USA

Kyle A. Rozman
National Energy Technology Laboratory
1450 Queen Avenue SW
Albany, OR 97321, USA

Ömer N. Doğan
National Energy Technology Laboratory
1450 Queen Avenue SW
Albany, OR 97321, USA

ABSTRACT

Internal corrosion in wet natural gas is a big challenge in the oil and gas industry due to corrosive constituents such as carbon dioxide (CO_2), hydrogen sulfide (H_2S), other forms of sulfur, and water in the gas stream. To mitigate internal corrosion, zinc-based cold spray coatings were designed for use in natural gas pipelines to increase the lifespan of the pipeline network. However, one of the requirements in designing internal coatings is the resistance of the coatings to mechanical forces applied on the pipeline's internal wall during pigging operations. These forces are primarily compressive and shear/friction forces. This study examines material properties that must be considered when evaluating mechanical considerations.

To determine the viability of the developed coatings with respect to the shear/friction forces, the shear adhesion and wear resistance of the materials have been evaluated. Shear adhesion testing was performed with modified clevises to determine the shear stress required to cause adhesion failure at the coating/substrate interface. Scanning electron microscopy was utilized to characterize the interfaces after failure. Wear testing was performed on coatings and pipeline materials utilizing pin-on-drum testing. These tests display the stress limitations and wear that the coatings can tolerate from pigging.

Keys words: cold spray coatings, zinc, wear test, steel pipelines, internal coatings

INTRODUCTION

Internal corrosion in wet natural gas is a big challenge in the oil and gas industry due to corrosive constituents such as carbon dioxide (CO_2), hydrogen sulfide (H_2S), other forms of sulfur, and water in the gas stream. To mitigate internal corrosion, zinc-based cold spray coatings were designed for use in natural gas pipelines to increase the lifespan of the pipeline network[1–3]. The cold spray technique comes with a number of benefits over other protective techniques, including: acting as a self-healing sacrificial protection, high bond strength, low oxygen content, lower temperature application, and thicker less pours coating layers[4,5]. The usefulness of an internal coating, however, must be able to stand up to the mechanical degradation that would occur.

Pipelines are an incredibly cost-effective method of transportation of fluids, both liquids and gases. Maintenance of pipelines (especially hazardous and/or toxic fluids) is important for safety, cost-effectiveness, reliability, lifespan, and resource management. Regular maintenance includes inspecting, repairing, and cleaning. Special equipment commonly referred to as pipeline pigs are utilized to perform these functions with minimal operational disruption.

Pigs used to maintain continuous operation and maximize efficiency perform tasks such as cleaning (remove debris, waxes, and contaminants) and inspecting (monitor and detect degradation such as cracks, dents, corrosion, etc.)[6]. Types of pigs used in maintenance can vary in form (foam, brush, disc, blade, seal, and various detectors); however, they are all most commonly driven through the pipelines using some form of differential pressure (Figure 1).

Driving pigs through pipelines creates multiple forces and pressures on both the pig and the pipeline. The primary forces acting on the pipe during pigging processes, and therefore any coatings, are displayed in Figure 1. The forces are split between wall (compressive) and friction (shear). The compressive forces are determined largely geometrically with respect to the differential pressure over the pig and the frictional coefficient[7]. As long as the pig is traveling at constant speed, the shear force is determined by the pig's driving force, the force due to pressure differential.

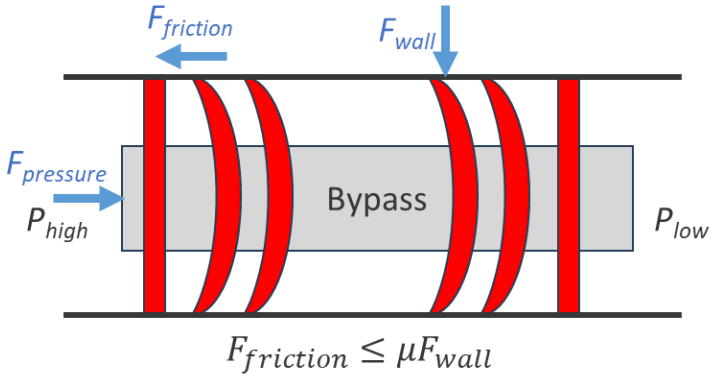

Figure 1: Forces imparted during pigging operations.

The differential pressure required to drive a pig can be estimated by Equation (**Eq. 1)**[6]. The differential pressure (DP) is calculated in bars from the type of pig (K) and the nominal diameter of the pipe in inches (d). The K-type pig referenced in Equation 1 has foam pigs as K=1; cup, cone, and discs pigs ranging from K=4-12; brush and blade on the order of K=12-15; ultrasonic in-line inspection tools as K=19; and magnetic flux leakage in-line inspection tools on the order of K=24. Equation (**Eq. 1)** is plotted to visualize the differential pressure required to drive different types of pigs which can be seen in Figure 2.

$$DP = \frac{K}{d}\ [bar] \qquad \textbf{(Eq. 1)}$$

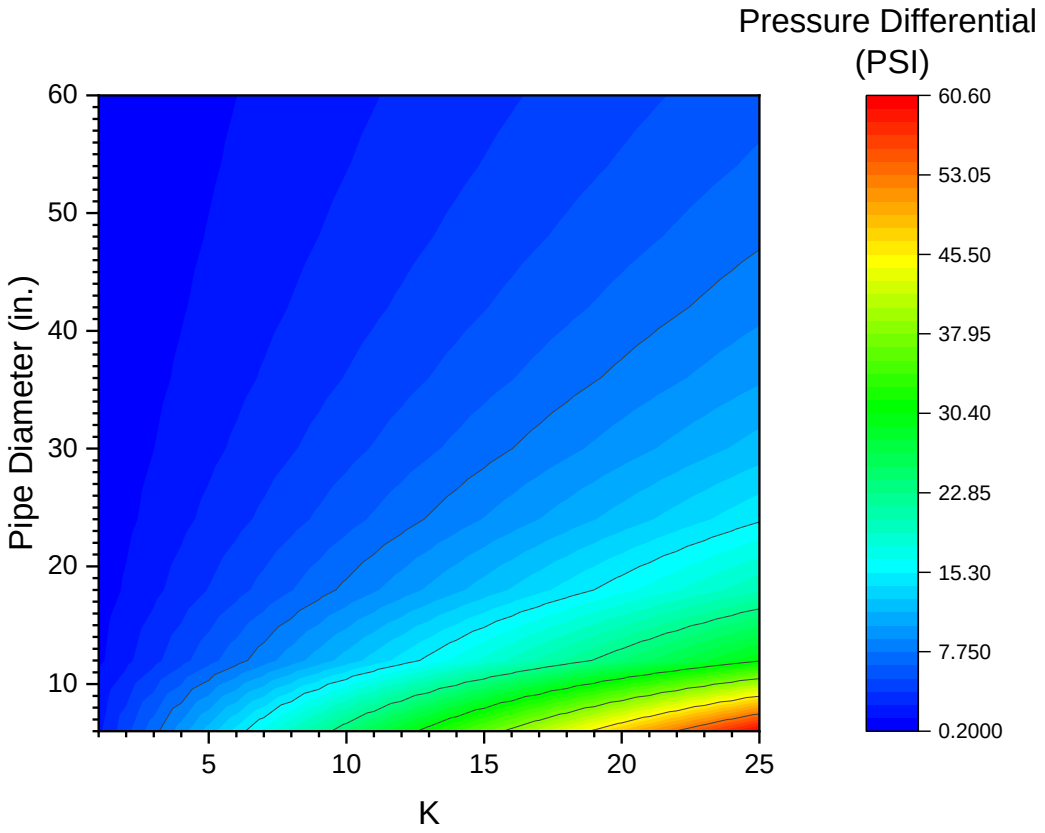

Figure 2: Differential pressure required to drive pigs by K-type.

The shear and wall forces that are imparted on the pipe wall, and thereby any coatings, will be distributed as axial and shear stresses (Figure 3). Since the loads applied during the pigging process will be shear and axial compression, delamination at the coating and pipeline interface would occur as a result primarily of shear stresses. There are many methods of testing adhesion and multiple methods of specifically testing the shear adhesion strength of an interfacial bond[8–10]; however, the shear adhesion testing revolves around two primary methodologies, shearing through tension or shearing through rotation. The adhesion testing should identify the bond strength and further identify if the bond failure was cohesive (within the adherend) or adhesive (at the interface)[11].

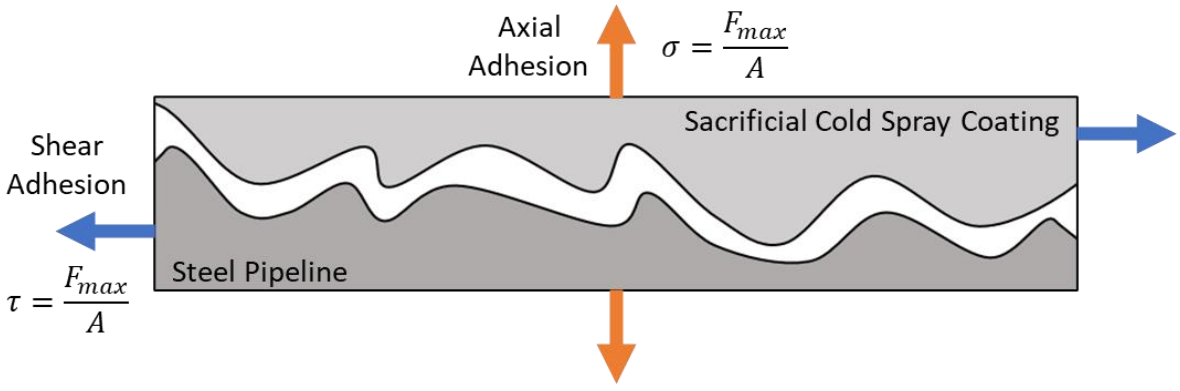

Figure 3: Adhesion axial vs. shear.

Pigging will also impart a significant degree of abrasive degradation onto the pipeline wall. This degradation specifically would entail the loss of surface material, and is related to the frictional force on the pipe wall (Figure 1), as well as the abrasivity of any tooling included on the pigs (such as cleaning brushes and scrapers). For a coating to be useful in these systems, they must survive periodic pigging,

meaning that the coatings must display acceptable levels of material loss during tribological testing. Benchmarking where coatings fall in comparison to known materials (such as the pipeline itself) would show how well the coatings would withstand typical operations.

Much of the scientific literature regarding wear in pipelines involves either research into wear of the pig itself[12–14] or the wear/erosion of the pipeline materials and/or coatings during regular operation[15,16]. The characterization of the wear resistance of the pipeline and the underlying coating has been standardized. The standards were developed with specific designs. Some were developed to evaluate specific types of wear, simulate a particular application, or evaluate a specific type of material. These methods include tests such as fretting, vibratory, cavitation, slurry abrasivity, galling, and pin abrasion testing[17]. The pin on abrasion testing method was developed to determine the wear resistance of a material during sliding[18,19]. The general method causes severe abrasion and does not duplicate all environmental specific conditions. Thus, this method is not utilized to predict specific wear rates of a material under usage conditions but rather provide a relative ranking of the abrasion resistance of materials.

To determine the viability of the developed coatings with respect to the shear/friction forces, the shear adhesion and wear resistance of two zinc-based cold spray coatings and comparative API 5L X65 and pure zinc have been evaluated.

EXPERIMENTAL PROCEDURE

Testing materials include two metals (API 5L steel X65 and pure zinc, both in Table 1), two zinc cold spray blends (ZnCr and ZnNb), and polytetrafluoroethylene. The volume fraction of additive in each the two cold spray coatings were 12.8±2.2 and 2.8±2.5 for ZnCr and ZnNb, respectively. Final thicknesses for the coatings were 340.2±7.0 and 428.4±5.1 µm for the ZnCr and ZnNb, respectively. The behavior of these coatings was previously characterized in earlier publications[1–3].

Table 1: Composition (wt.%) Base Metals

Elements	C	Mn	P	S	Al	Cr	Cu	Mo	Nb	Ni	Si	Zn	Fe
Zinc	**-**	-	-	-	<0.5	-	<0.005	-	-	-	-	Bal.	<0.005
X65	0.08	1.17	0.009	0.003	-	0.018	0.011	0.001	0.001	0.013	0.2	-	Bal.

Adhesion Testing

Adhesion testing was conducted on the cold spray ZnCr/steel and ZnNb/steel interfaces. Axial adhesion testing was previously conducted on the cold spray interfaces following ASTM C633[20]. Shear adhesion testing was conducted following the methodology in ASTM B831[21]; however, the geometry of the sample

was altered to accommodate the nature of the coating testing. Specifically, jigs were created to hold

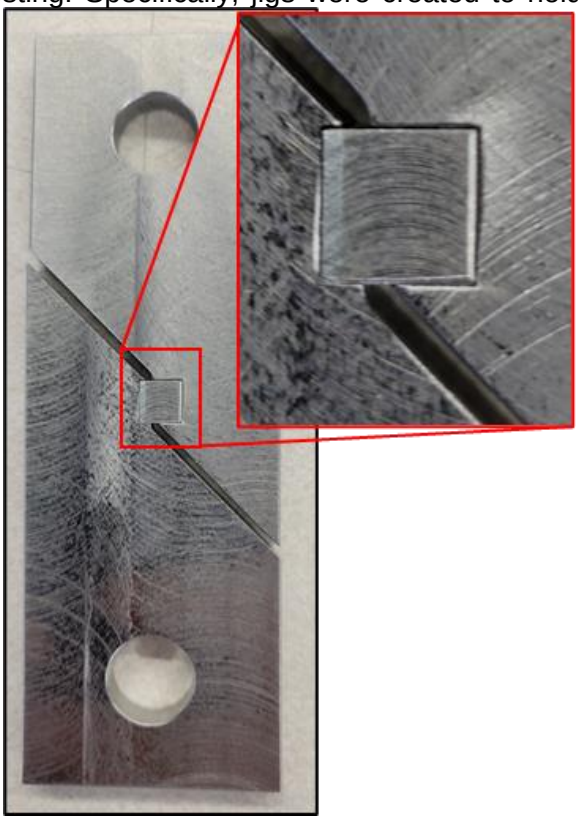

"coating cubes." The jig with a sample cube is displayed in Figure **4:Shear adhesion testing sample geometry.**

Utilizing the maximal force measured, and sample interfacial area, the shear adhesion strength was calculated using Equation (**Eq. 2**. In the calculation, $F_{t,max}$ is the maximum force recorded to shear the coating from the substrate, and A is the cross-sectional area of the coating/steel interface. The calculation for axial adhesion strength is the same with the forces acting on the interface being normal ($F_{n,max}$) instead of tangential, Equation (**Eq. 3)**.

$$\tau = \frac{F_{t,max}}{A} \quad [MPa] \qquad \textbf{(Eq. 2)}$$

$$\sigma = \frac{F_{n,max}}{A} \quad [MPa] \qquad \textbf{(Eq. 3)}$$

After mechanically shearing the cold spray coating and steel interface, the newly exposed surfaces of both sections were examined in order to ensure adhesive failure. The two surfaces were cleaned using an ultrasonication and isopropanol for 10 minutes in order to remove any residual oils from mechanical testing and handling. The surfaces were examined using a scanning electron microscope (SEM) with energy dispersive X-ray spectroscopy (EDS) in order to visually analyze the surface and to chemically characterize the two interface surfaces. Ideally, it would be characterized as either a structural, adhesive, or cohesive failure. Additionally, in the event of adhesive failure, there are often areas of detached coating/substrate that remain with the opposing interface. This imperfect adhesion testing behavior is displayed in Figure 5, where mechanical interlocking of the coating and the substrate can cause shearing. Using EDS to chemically map the two surfaces of the exposed interface, the amount of opposing material left on each surface was analyzed. Using ImageJ, the area fraction of iron on the coating surface and the area fraction of cold spray on the steel surface were calculated.

. Sample cubes were machined to cubes of 0.25" edge length with an additional 0.04" coating on one edge surface. The tests were conducted in a 5882 Instron test frame with a 25kN testing capacity and

5800-control system was used for the mechanical testing. An extension rate of 0.0077 mm/min was utilized until ultimate sample delamination.

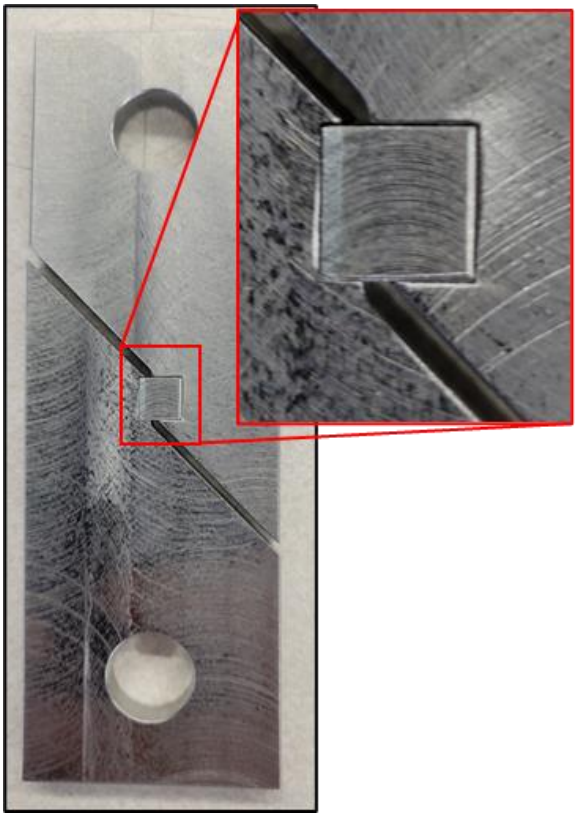

Figure 4:Shear adhesion testing sample geometry.

Utilizing the maximal force measured, and sample interfacial area, the shear adhesion strength was calculated using Equation (**Eq. 2**. In the calculation, $F_{t,max}$ is the maximum force recorded to shear the coating from the substrate, and A is the cross-sectional area of the coating/steel interface. The calculation for axial adhesion strength is the same with the forces acting on the interface being normal ($F_{n,max}$) instead of tangential, Equation (**Eq. 3)**.

$$\tau = \frac{F_{t,max}}{A} \quad [MPa] \qquad \textbf{(Eq. 2)}$$

$$\sigma = \frac{F_{n,max}}{A} \quad [MPa] \qquad \textbf{(Eq. 3)}$$

After mechanically shearing the cold spray coating and steel interface, the newly exposed surfaces of both sections were examined in order to ensure adhesive failure. The two surfaces were cleaned using an ultrasonication and isopropanol for 10 minutes in order to remove any residual oils from mechanical testing and handling. The surfaces were examined using a scanning electron microscope (SEM) with energy dispersive X-ray spectroscopy (EDS) in order to visually analyze the surface and to chemically characterize the two interface surfaces. Ideally, it would be characterized as either a structural, adhesive, or cohesive failure. Additionally, in the event of adhesive failure, there are often areas of detached coating/substrate that remain with the opposing interface. This imperfect adhesion testing behavior is displayed in Figure 5, where mechanical interlocking of the coating and the substrate can cause shearing. Using EDS to chemically map the two surfaces of the exposed interface, the amount of opposing material

left on each surface was analyzed. Using ImageJ, the area fraction of iron on the coating surface and the area fraction of cold spray on the steel surface were calculated.

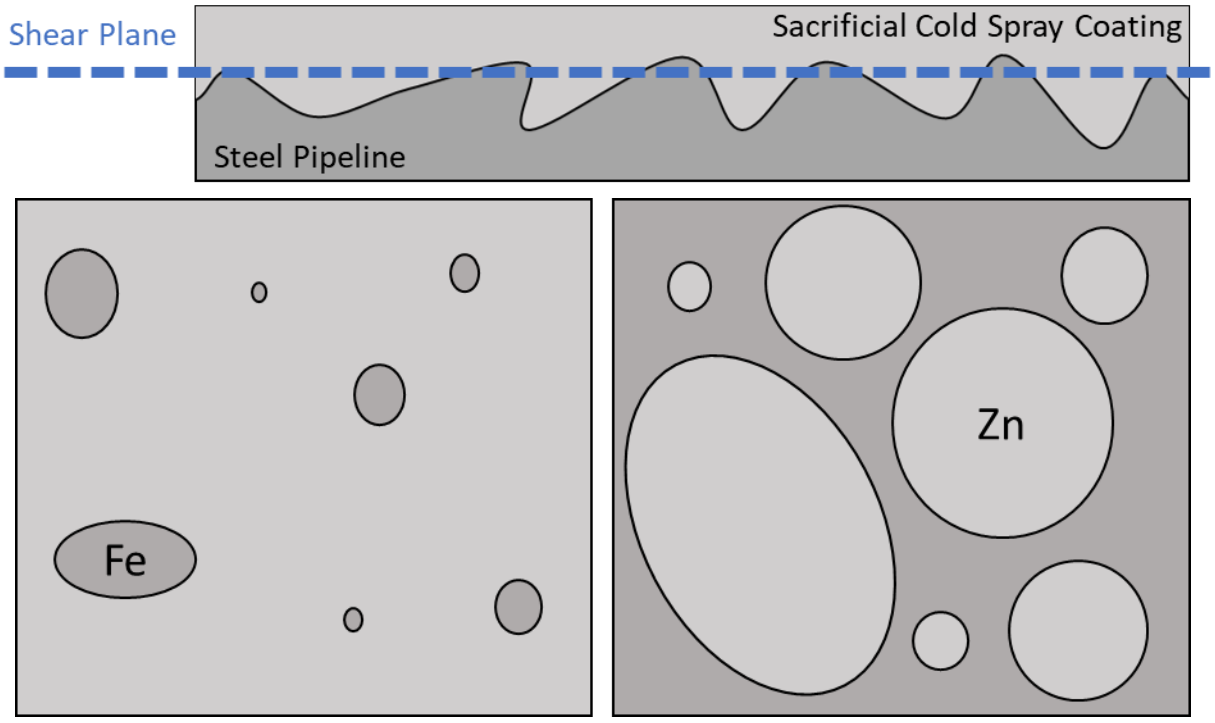

Figure 5: The two interface surfaces developed from splitting at the (a) shear plane where the two interfaces delaminate with (b) fractions of the iron detach from the steel base material and remain with the coating, and (c) fractions of the cold spray detach from the coating and remain with the steel.

Wear Testing

Wear testing was conducted on the following materials: steel X65, zinc, cold spray coating ZnCr, cold spray coating ZnNb, and polymer polytetrafluoroethylene. Wear testing utilizing a pin-on-drum testing methodology was conducted following ASTM G132[18]. The setup displayed in Figure 6 shows a sample loaded into a weighted chuck transversing perpendicular across the drum while both the sample and the drum are rotating. All rotation and traverse speeds were constant. The traverse speed and drum rotational speed were set so that a double helix path could be created where both the testing sample and the reference sample could traverse the same length of the abrasive without overlapping.

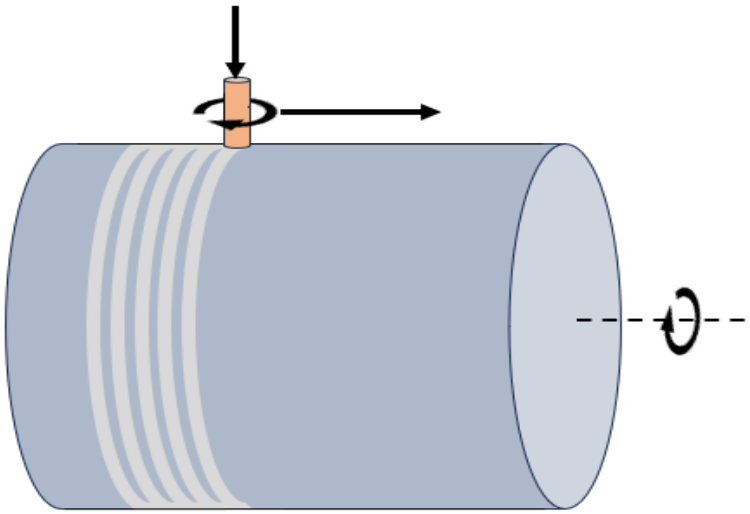

Figure 6: Pin-on-drum wear testing setup with a loaded sample traversing a rotating drum.

The tests were conducted using 150-grit SiC sandpaper adhered to the drum. The force exerted on the ¼" rotating pins was set to impart a contact pressure of 1 MPa (a force of 65.47 N) for a travel distance of 3.2 m. These tests compared multiple materials for use in pipelines. The calculation for the wear rate of a material is displayed in Equation (**Eq. 4**. The wear rate is calculated by using the mass loss of the sample from before and after the test, W_x; its known density, ρ, the mass loss of a reference specimen, S_x; and the mean mass loss per travel distance per load of the reference material over a large number of tests for the abrasive type and test parameters used, C. The mean loss value C utilized in this calculation and for these parameters and equipment was 0.1814 $[mg/N \cdot m]$. The C:S_x ratio is a normalizing factor in the equation. Each material was tested three times in order to statistically determine the wear rate.

$$wear = \frac{C\ W_x}{\rho\ S_x} \quad \left[mm^3/_{Nm}\right] \qquad \textbf{(Eq. 4)}$$

Pins were examined with the SEM, both in the worn and unworn state, to confirm that only the coating material was removed during the wear testing of the coating materials. Sufficient coating remained after testing, confirming that the steel the coating was adhered to did not affect the wear test. The wear surfaces were examined as well, in order to determine if the additives' particles of the metallic coatings were disproportionally removed from the surface during wear testing. Aside from wear tracts, there was not sufficient evidence to indicate there is a significant difference in particle distribution pre- and post-wear testing.

RESULTS

Adhesion Testing

The shear adhesion strength was calculated for each material by examining the ultimate tensile strength. Figure 7 is an example force/displacement plot of one of the tests and is representative of the behavior of the other tests conducted. The ultimate force before failure was recorded for each test and the shear adhesion strength was calculated utilizing Equation (**Eq. 2**. Shear adhesion values for ZnCr (15.3 ± 1.5 MPa) and ZnNb (9.7 ± 2.1 MPa) were plotted in Figure 9, where the shear adhesion and area fractions of interfacial remnants are compared.

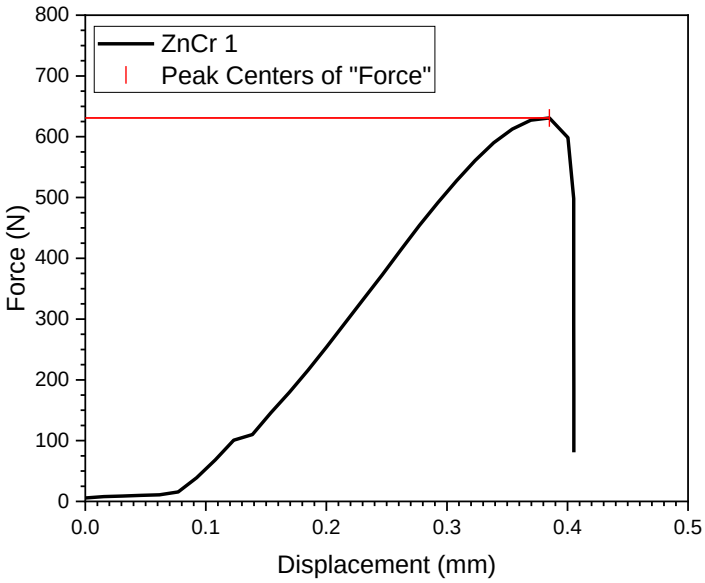

Figure 7: Maximum tensile stress for ZnCr/steel interface for replicate #1.

The EDS chemical maps of each surface are displayed in Figure 8. The intensity maps display the areas of the surface that contain the opposing material. Using ImageJ to mask and calculate the area fraction, it is evident that the area fraction of iron left on the coating was 8.2% and 4.4% for the ZnCr and ZnNb coatings, respectively. The area fraction of coating left on the steel substrate was 22.2% and 12.1%, respectively. These values are plotted in Figure 9 as green and purple for the iron and cold spray detected on the surface, respectively. In both cases, there was significantly more cold spray left on the steel substrate than vice versa. This is due to the individual coating vs. cold spray strengths. With lower strength than the steel substrate, a larger portion of the coating would remain on the steel surface.

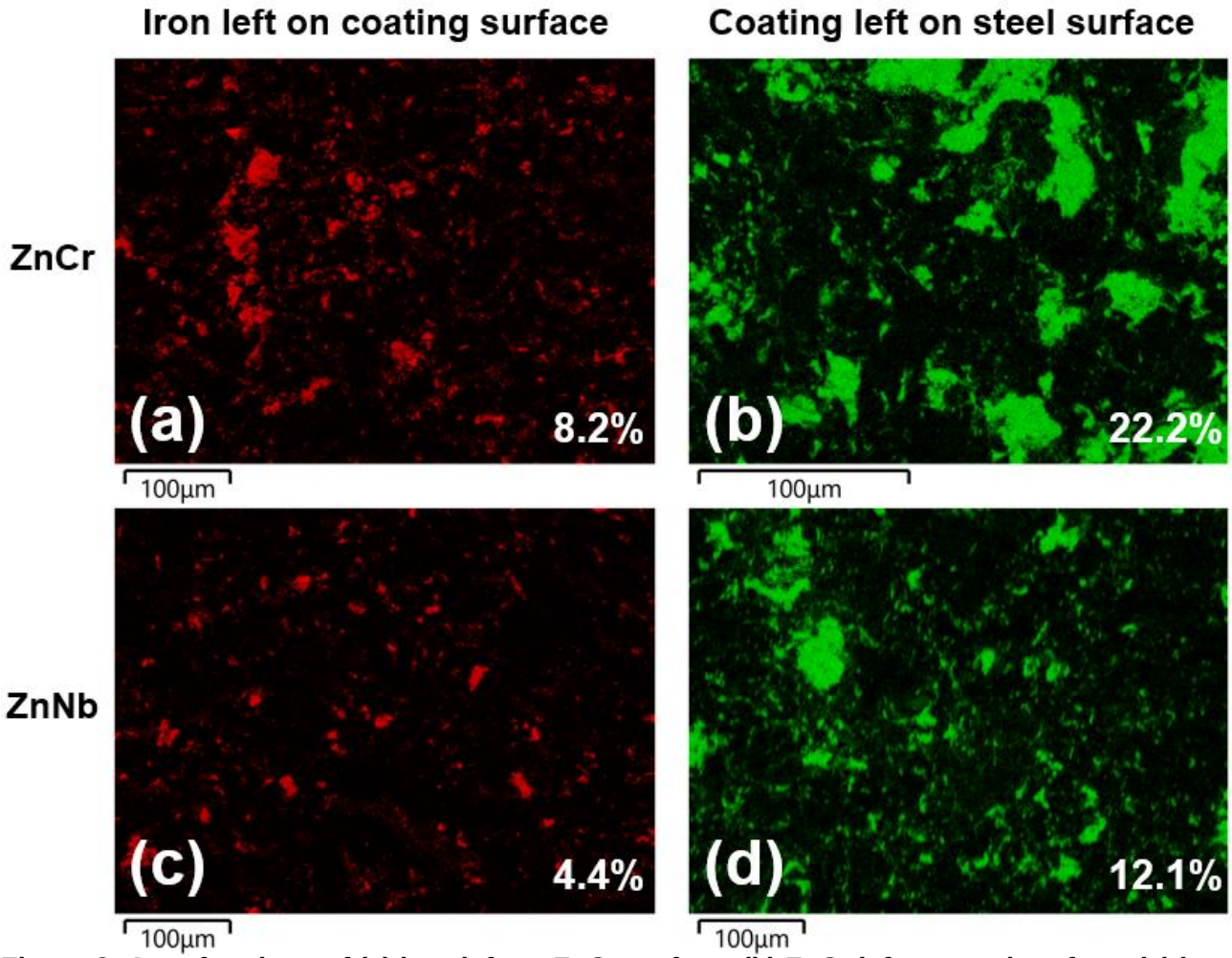

Figure 8: Area fractions of (a) iron left on ZnCr surface, (b) ZnCr left on steel surface, (c) iron left on ZnNb surface, and (d) ZnCr left on steel surface.

The shear adhesion testing and area fractions detected are plotted together in Figure 8. Each value has its own y-axis scale. The three datasets for each cold spray coating were scaled individually to show the apparent relationship between the shear adhesion and the area fraction of the opposing material left on an interfacial surface. From the data shown in Figure 8, it was observed that the mechanical interlocking and that occurred with the coatings and the degree of material left behind was related to the shear strength measured. It appears that the ZnCr coating had better mechanical interlocking and thus developed a larger shear adhesion strength in comparison to the ZnNb coating.

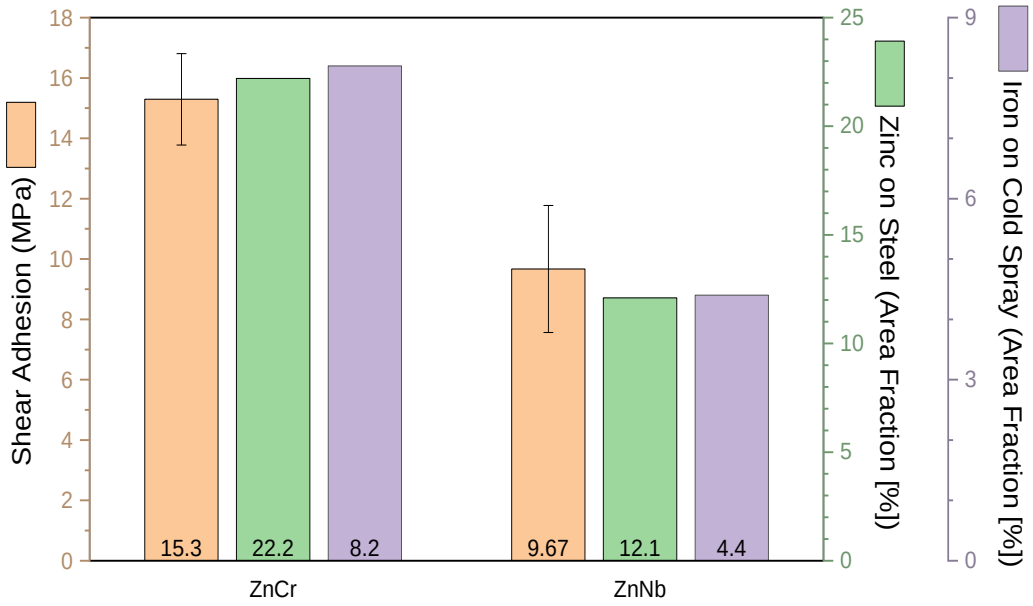

Figure 9: Shear adhesion (orange) and interfacial fractions of the coating embedded on steel surface (green) and of the steel embedded in the cold spray surface (purple).

If these coatings are to be used in pipelines, the forces imparted by any pigging operations should remain at a level where the imparted stresses at the interface remain well below the 15 and 9.7 MPa shear stress that was measured for the ZnCr and ZnNb cold spray coatings, respectively. When examining Equation 1 and considering a large K-type pig (24) and a typical diameter pipe (6”) we can see that it requires a 0.4 MPa pressure differential equating to an approximate 7 kN driving force, which is balanced by the frictional force. In order to remain under the 9.7 MPa shear stress required for the ZnNb coating, the ~7 kN frictional force would need to be spread over at least 1.2 in^2 along the pig. The frictional area required to remain under the shear stress is proportional to the K-type of pig and to the diameter of the pipe. With a 24 K-type pig, the minimum area needed to spread the frictional forces for the ZnNb not to shear from the pipe wall would be greater than 0.59 in^2 for a 3” diameter pipe and 7 in^2 for a 3’ diameter pipe.

Wear Testing

The wear testing was conducted on coating specimens with thin coatings. Therefore, to ensure that the tests were valid, SEM was conducted pre and post testing to ensure that the coating remained intact and only the coating material was removed. SEM backscatter images (Figure 10) show the sideview of two representative wear pins. In backscatter images (where contrast is dependent on atomic density), the lighter top layer is the less atomically dense cold spray coating and the darker layer is more atomically dense steel. For both coatings, before (Figure 10 a and c) and after (Figure 10 b and d) the wear testing, it can be determined that the wear test results did not contain steel substrate interference.

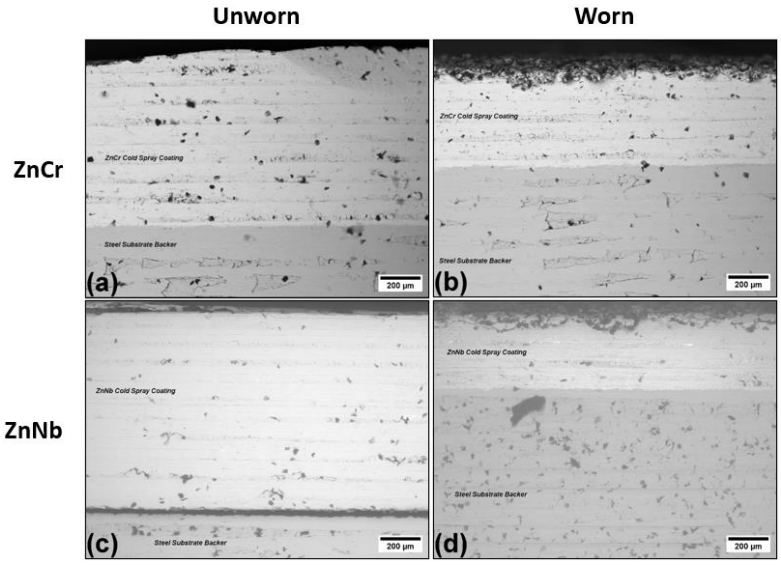

Figure 10: Side view of wear pins with cold spray coating bonded to the steel substrate for a pin both (a) pre-worn ZnCr, (b) ZnCr after wear, (c) pre-worn ZnNb, and (d) ZnNb after wear.

The wear testing results, displayed in Figure 11, where the ZnCr and ZnNb cold spray coatings were compared to a pipeline steel and a polymer-based coating. The results show very similar behavior between pure zinc and the two different zinc-based cold spray coatings. Cold spray ZnCr performs slightly better than the ZnNb cold spray. The wear rate for zinc ($8.01 \times 10^{-2} \pm 1.04 \times 10^{-3}$ *mm³/Nm*), ZnCr ($8.19 \times 10^{-2} \pm 1.14 \times 10^{-3}$ *mm³/Nm*), and ZnNb ($8.69 \times 10^{-2} \pm 0.87 \times 10^{-3}$ *mm³/Nm*) are all approximately three times greater than that of the steel X65 ($2.49 \times 10^{-2} \pm 2.09 \times 10^{-3}$ *mm³/Nm*). In contrast, the wear rate of zinc and the zinc-based cold spray coatings was nine times lower than the polytetrafluoroethylene ($7.22 \times 10^{-1} \pm 6.51 \times 10^{-2}$ *mm³/Nm*). This shows that while pigging operations would incur more wear on the coating than the base pipe would experience, it is an order of magnitude less wear than the comparative polymer-based coating in this study.

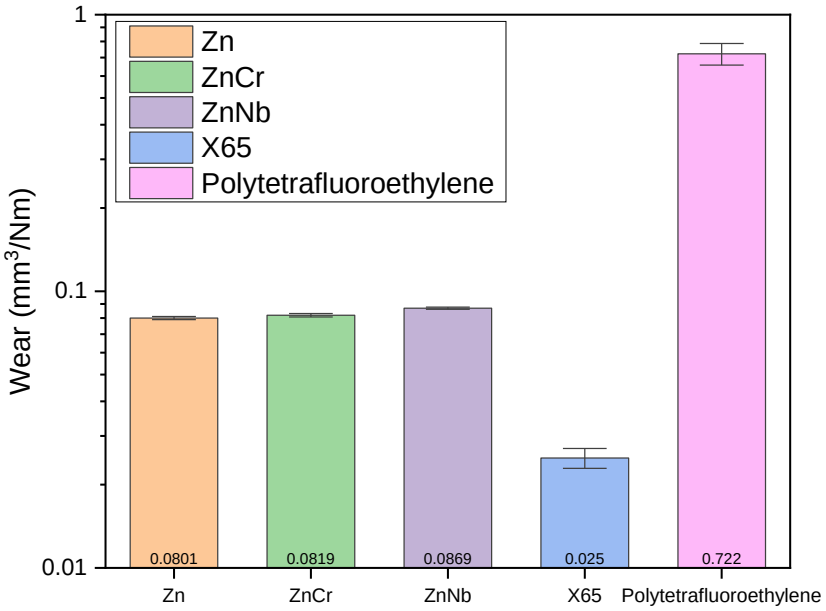

Figure 11: Wear rates with 150-grit SiC sandpaper under 1 MPa.

CONCLUSIONS

The viability of the developed coatings has been evaluated with respect to the shear/friction forces, the shear adhesion, and wear resistance. The materials that were tested for adhesion were ZnCr and ZnNb cold spray coatings adhered to a steel backer. The shear adhesion testing revealed that the ZnCr cold spray sheared at 15.3 ± 1.5 MPa and the ZnNb cold spray sheared at 9.7 ± 2.1 MPa. The percentage of flaked substrate left behind at each interface was proportional to the shear stress at failure.

Wear testing of the two metals (API 5L steel X65 and pure zinc), two zinc-based cold spray blends (ZnCr and ZnNb), and polytetrafluoroethylene was carried out to determine the viability of the coatings with respect to tribology. The two zinc-based cold spray coatings performed similarly to the pure zinc material. The zinc-based cold spray coatings had wear rates of $8.19 \times 10^{-2} \pm 1.14 \times 10^{-3}$ mm^3/Nm for ZnCr and $8.69 \times 10^{-2} \pm 0.87 \times 10^{-3}$ for ZnNb. The wear rate for pure zinc was $8.01 \times 10^{-2} \pm 1.04 \times 10^{-3}$ mm^3/Nm. These three zinc-based materials had a wear rate approximately three times greater than X65 with a wear rate of $2.49 \times 10^{-2} \pm 2.09 \times 10^{-3}$ mm^3/Nm. The three zinc-based materials conversely had a wear rate an order of magnitude lower than the polymer polytetrafluoroethylene, $7.22 \times 10^{-1} \pm 6.51 \times 10^{-2}$ mm^3/Nm.

The differential pressure needed to drive even the more robust of cleaning pigs is unlikely to cause sufficient shear forces that the interfacial adhesion would be compromised during typical cleaning pigging operations. It is unlikely that these coatings would delaminate from pipelines due to mechanical forces. The wear rate results from pin-on-drum testing showed promising results. Both of the zinc-based cold spray coatings were less resistant to wear than the base pipeline material; however, they were an order of magnitude more resistant than a representative polymer coating. Both shear adhesion testing and pin-on-drum wear testing have demonstrated that these coatings have the potential to be utilized in pipelines where regular pigging is performed. However, more testing with simulated systems would likely be necessary.

ACKNOWLEDGEMENTS

This work was performed in support of the U.S. Department of Energy's (DOE) Office of Fossil Energy and Carbon Management's Methane Mitigation Technology Research Program and executed through the National Energy Technology Laboratory's (NETL) Research & Innovation Center's Natural Gas Infrastructure Field Work Proposal.

The researchers would like to thank Trevor Godell for machining of specimens and Chris Powell for assistance with mechanical testing.

DISCLAIMER

REFERENCES

1. Teeter, L., M. Ziomek-Moroz, J. Tylczak, and G. Crawford, "ZnCr and ZnNb Cold Spray Coatings," in CORROSION2021 (NACE, 2021).
2. Belarbi, Z., R.E. Chinn, and O.N. Dogan, "Corrosion Behavior of Zinc Cold Spray Coatings (ZnCr & ZnNb) in a Simulated Natural Gas Environment Containing H2O, CO2, and H2S," in AMPP 2024 (New Orleans: AMPP, 2024).
3. Belarbi, Z., Richard.E. Chinn, and Ö.N. Doğan, *Corrosion* 80 (2024): pp. 676–692.
4. Revie, R.W., and H.H. Uhlig, *Corrosion and Corrosion Control: An Introduction to Corrosion Science and Engineering*, 4th ed. (John Wiley & Sons, Inc, 2008).
5. Karthikeyan, J., *The Cold Spray Materials Deposition Process: Fundamentals and Applications* (2007): pp. 62–71.
6. Cordell, Jim., and Hershel. Vanzant, *The Pipeline Pigging Handbook* (Clarion Technical Publishers, 2003).
7. den Heijer, A., "Frictional Behaviour of Pigs in Motion," Master of Science, Delft university of Technology, 2016, http://repository.tudelft.nl/.
8. Maxwell, A.S., "Review of Test Methods for Coating Adhesion" (2001).
9. Jouan, A., and A. Constantinescu, *Int J Adhes Adhes* 84 (2018): pp. 63–79.
10. Era, H., F. Otsubo, T. Uchida, S. Fukuda, and K. Kishitake, *Materials Science and Engineering: A* 251 (1998): pp. 166–172.
11. Marshall, S.J., S.C. Bayne, R. Baier, A.P. Tomsia, and G.W. Marshall, *Dental Materials* 26 (2010): pp. e11–e16.
12. Zhu, X., S. Zhang, X. Li, D. Wang, and D. Yu, *J Nat Gas Sci Eng* 23 (2015): pp. 127–138.
13. Zhang, H., C. Sanchez, S. Liu, S. Zhang, and H. Liang, *J Nat Gas Sci Eng* 41 (2017): pp. 40–48.
14. Hendrix, M.H.W., C.M. Graafland, and R.A.J. van Ostayen, *J Pet Sci Eng* 171 (2018): pp. 905–918.
15. Okonkwo, P.C., R.A. Shakoor, E. Ahmed, and A.M.A. Mohamed, *Eng Fail Anal* 60 (2016): pp. 86–95.

16. Shemyakinskiy, B., A. Lamonov, V. Yakhimovich, and O. Shvetsov, *Mater Today Proc* 30 (2020): pp. 578–582.
17. Blau, P.J., and K.G. Budinski, *Wear* 225–229 (1999): pp. 1159–1170.
18. ASTM International, “ASTM G132: Standard Test Method for Pin Abrasion Testing” (1996).
19. ASTM International, “ASTM G99: Standard Test Method for Wear Testing with a Pin-on-Disk Apparatus” (2000).
20. ASTM International, “ASTM C633: Standard Test Method for Adhesion or Cohesive Strength of Flame-Sprayed Coatings” (1993).
21. ASTM International, “ASTM B831: Standard Test Method for Shear Testing of Thin Aluminum Alloy Products” (2005), www.astm.org,.